*Work supported by a National Research Council of Canada Grant No. A2883.

[1]F. J. Morin, Phys. Rev. 78, 819 (1950); A. H. Morrish, G. B. Johnston, and N. A. Curry, Phys. Letters 7, 177 (1963).
[2]C. G. Shull, W. A. Strauser, and E. O. Wollan, Phys. Rev. 83, 333 (1951).
[3]I. Dzialoshinskii, Zh. Eksperim. i Teor. Fiz. 32, 1547 (1957) [Soviet Phys. JETP 5, 1259 (1957)].
[4]T. Moriya, Phys. Rev. 120, 91 (1960).
[5]P. J. Besser, A. H. Morrish, and C. W. Searle, Phys. Rev. 153, 632 (1967).
[6]C. W. Searle, Phys. Rev. Letters 21, 741 (1968).
[7]J. A. Eaton, A. H. Morrish, and C. W. Searle, Phys. Letters 26A, 520 (1968).
[8]R. Nathans, S. J. Pickart, H. A. Alperin, and P. J. Brown, Phys. Rev. 136, A1641 (1964).
[9]G. Cinader and S. Shtrikman, Solid State Commun. 4, 459 (1966).
[10]F. van der Woude, Ph. D. thesis, University of Groningen, Holland, 1966 (unpublished).
[11]P. J. Flanders and S. Shtrikman, Solid State Commun. 3, 285 (1965).
[12]T. Moriya, in *Magnetism I*, edited by G. T. Rado and H. Suhl (Academic, New York), pp. 97, 92, 93.
[13]J. O. Artman, J. C. Murphy, and S. Foner, Phys. Rev. 138, A912 (1965).
[14]G. Cinader, P. J. Flanders, and S. Shtrikman, Phys. Rev. 162, 419 (1967).
[15]C. W. Searle, Phys. Letters 25A, 256 (1967).
[16]H. Umebayashi, B. C. Frager, and G. Shirane, Phys. Letters 22, 407 (1966).
[17]T. G. Worlton, R. B. Bennion, and R. M. Brugger, Phys. Letters 24A, 653 (1967).
[18]J. Kanamori and H. Minatono, J. Phys. Soc. Japan 17, 1759 (1962).
[19]P. J. Flanders, J. Appl. Phys. 40, 1247 (1969).
[20]V. I. Ozhogin, S. S. Yakimov, R. A. Voskanyan, and V. Ya. Gamlickii, Institute of Atomic Energy Report No. IAE 1674, Moscow, 1968 (unpublished).
[21]D. C. Herbert, Ph. D. thesis, London University, 1968 (unpublished).

PHYSICAL REVIEW B VOLUME 1, NUMBER 11 1 JUNE 1970

Harmonic Generation and Parametrically Coupled Spin Waves in Yttrium Iron Garnet*

J. D. Bierlein† and Peter M. Richards
Department of Physics, University of Kansas, Lawrence, Kansas 66044
(Received 30 December 1969)

Second-harmonic generation and ferromagnetic resonance have been investigated in spheres of yttrium iron garnet (YIG) as a function of incident power above the threshold for excitation of z-directed spin waves by the second-order Suhl instability. The fundamental frequency was 8.42 GHz and the temperature 300 °K. The second-harmonic power output $P_{2\omega}$ has the following features above threshold: (a) $P_{2\omega}$ goes through a minimum and then a maximum as a function of incident power; (b) the line profile of $P_{2\omega}$ versus dc field H shows two and then three peaks; (c) sufficiently far above threshold, $P_{2\omega}$ initially increases after the pulse of incident power is turned off. None of these effects is correlated with unusual behavior of the transverse magnetization, which always increases with power above threshold, has a single resonance line, and begins to decay as soon as incident power is turned off. The results are explained in terms of parametric coupling between the initially excited z-directed spin waves and other spin waves, with explicit account taken of the ensuing phase relations. These tend to make the other spin waves interfere destructively with the uniform mode ($k=0$) in their contribution to $P_{2\omega}$. In this way, quantitative agreement between theory and experiment is obtained with reasonable values for two adjustable parameters. Coherent phase relations between the interacting spin waves are essential for an understanding of the results. If all $k \neq 0$ magnon interactions are lumped into effective relaxation rates, it is possible to explain the transverse resonance data, but not the second-harmonic effects.

I. INTRODUCTION

Since the explanation by Suhl[1] of the premature saturation of ferromagnetic resonance observed by Bloembergen and Wang,[2] it has been known that spin waves of nonzero wave vector are excited in conventional (transverse pumping) ferromagnetic resonance experiments. This excitation occurs through parametric coupling of the uniform mode to a pair of spin waves with wave vectors $\vec{k}$ and $-\vec{k}$. When the uniform mode reaches a critical amplitude determined by the coupling strength and spin-wave relaxation rate, the pair $\vec{k}$ and $-\vec{k}$ is excited to a very large amplitude. Further growth of the uniform mode amplitude is inhibited, thus causing the observed saturation.

In its original and most elementary form, theory predicts the uniform-mode amplitude to stay constant above threshold which results in the rf susceptibility declining as $1/h$, where h is the driv-

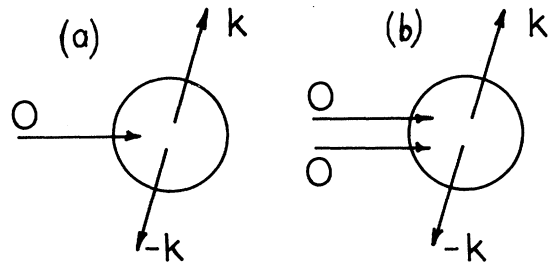

FIG. 1. (a) First-order Suhl process. A uniform mode ($k=0$) magnon is destroyed and a pair $\vec{k}$, $-\vec{k}$ of nonzero wave-vector magnons is created. Conservation of energy requires $\omega_k=\frac{1}{2}\omega_0$, and this is possible in a YIG sphere at room temperature on resonance only for $\omega_0/2\pi>3.3$ GHz. (b) Second-order Suhl process. Two uniform-mode magnons are destroyed and a pair $\vec{k}$, $-\vec{k}$ of nonzero wave-vector magnons is created with $\omega_k=\omega_0$. It is always possible to satisfy this condition on resonance.

ing field amplitude. This has been verified[1,3,4] for the first-order Suhl process, which is illustrated in Fig. 1(a). For the second-order Suhl process, shown in Fig. 1(b), however, the susceptibility falls off more slowly than $1/h$. Such behavior occurs[5] even in highly pure, highly polished samples of yttrium iron garnet (YIG) where two-magnon scattering is not overly important.[6]

In this paper we report experiments on both the uniform mode and second-harmonic generation in a single-crystal YIG sphere above the second Suhl threshold. The results are interpreted as showing that the originally excited spin waves $\vec{k}$, $-\vec{k}$ grow to sufficiently large amplitude that they excite other spin waves by parametric coupling, as illustrated in Fig. 2. Striking effects on the second-harmonic power output – both steady state and transient – and second-harmonic line shape are explained in terms of coherent phase relations between these other spin waves and the original ones.

That spin waves other than the first ones to go unstable can be excited is certainly no surprise. The noteworthy feature of our results is the importance of phase relations among the various spin waves. Such phase coherences are not required in order to explain the behavior of ferromagnetic resonance, but they play a dominant role in harmonic generation.

In order to discuss the effects of coherent and incoherent phases (and precisely what we mean by these terms), consider some of the basic equations involving the second Suhl threshold and harmonic generation. {We assume throughout that the first Suhl process [Fig. 1(a)] is forbidden, which is the case in our experiments on YIG at X band.} The $k\neq0$ spin-wave amplitude c_k satisfies the equation

$$\dot{c}_k=-i\omega_k c_k-ig_{0k}c_0^2c_{-k}^\dagger+(\text{other terms})\ , \qquad (1)$$

where ω_k is the spin-wave frequency and g_{0k} is the coupling constant for destruction of two uniform mode ($k=0$) magnons and creation of the pair $\vec{k}$, $-\vec{k}$ [Fig. 1(b)]. The second term in (1) is recognized as arising from the Hamiltonian appropriate to Fig. 1(b):

$$\mathcal{H}(\text{Suhl second order})=g_{0k}^*c_0^{\dagger2}c_kc_{-k}+\text{H.c.}, \qquad (2)$$

where H.c. stands for "Hermitian conjugate" and the c's and $c^\dagger$'s are treated as boson annihilation and creation operators, respectively. The "other terms" in (1) describe all other scattering processes in which the mode $\vec{k}$ is involved. These may include coupling with phonons as well as with other $k\neq0$ magnons. A common assumption is to say that the only important effects of these other terms are to produce a frequency shift and finite lifetime. Thus (1) is approximated by

$$\dot{c}_k=i\tilde{\omega}_kc_k-\eta_kc_k-ig_{0k}c_0^2c_{-k}^\dagger\ , \qquad (3)$$

where $\tilde{\omega}_k$ is the shifted frequency and η_k is the relaxation rate. The standard assumptions required for the validity of rate equations must be employed in going from (1) to (3). These include random phases among the interacting spin waves and smallness of all $k\neq0$ spin-wave amplitudes compared to the one in question. When we say that $k\neq0$ spin waves have "incoherent phase relations" we henceforth mean that Eq. (3) is satisfied for all spin waves excited to appreciable amplitude. This term will be further clarified momentarily.

Solutions of (3) and a similar equation for $\dot{c}_{-k}^\dagger$ show[1,7,8] that c_k grows exponentially for $g_{0k}|c_0|^2>\eta_k$, assuming $\omega_k=\omega_0$. Steady-state conditions require, for $|c_k|^2\neq0$,

$$|c_0|^2=\eta_k/g_{0k}\ , \qquad (4)$$

which leads to the result that the uniform-mode amplitude remains constant above threshold. Another useful steady-state relation is

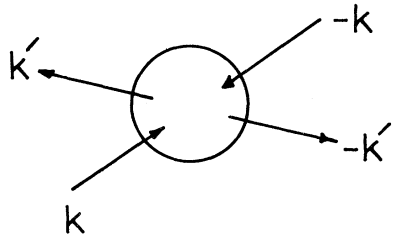

FIG. 2. Destruction of the magnons $\vec{k}$, $-\vec{k}$ created by the Suhl second-order process. For sufficiently large amplitudes of $\vec{k}$ and $-\vec{k}$, the pair can break up into another pair $\vec{k}'$, $-\vec{k}'$ by the same type of mechanism which limits the uniform mode [Fig. 1(b)].

$$c_k^\dagger c_{-k}^\dagger = i(g_{0k}^*/\eta_k)c_0^{\dagger 2}\,|c_k|^2 \tag{5}$$

for $|c_k|^2 \neq 0$. Thus there is a coherent phase relation between the magnons $\vec{k}$ and $-\vec{k}$. This results from the fact that $\vec{k}$ and $-\vec{k}$ are excited at the same time by the destruction of uniform-mode magnons.

Instead of saying that (3) implies incoherent phases, one could more properly state that the phases of $\vec{k}$ and $-\vec{k}$ are related by (5). That is, all excited spin-wave pairs have phases such that they absorb energy from the uniform mode. However, as seen, this does imply that interactions among $k \neq 0$ spin waves may be treated by effective relaxation rates without worrying about the relative phases of $\vec{k}$ and $\vec{k}'$ when $\vec{k}'$ is excited by scattering from $\vec{k}$.

It is not difficult to account for $|c_0|^2$ increasing above threshold within the framework of (4). As the initially excited spin waves grow in amplitude and the temperature of the magnon system increases, it is reasonable that the relaxation rate η_k will increase. This allows $|c_0|^2$ to increase according to (4). Schlömann[9] has used this same reasoning to discuss parallel-pump susceptibilities. It appears to work quite well in describing the transverse resonance susceptibility when the Suhl second-order process is operative, as we show in Sec. IV A. One might then ask why $|c_0|^2$ does remain constant above threshold for the first-order process. The Appendix is devoted to this question.

The above gives justification for the earlier statement that it is not necessary to consider phase relations among the excited spin waves for a description of the resonance susceptibility. These relations, however, are important to harmonic generation, as we now show.

The z component of magnetization, where z is the equilibrium direction, varies at a frequency 2ω if the transverse magnetization precesses in an elliptical path at frequency ω. With suitable microwave circuitry, this time variation can be detected in the form of second-harmonic power radiated from the sample. Ayres, Vartanian, and Melchor[10] first observed harmonic generation from the uniform mode. Richards and Shaw[11] later showed that $k \neq 0$ spin waves also contribute to harmonic generation.

The pertinent equations for describing second-harmonic generation are as follows:

$$M_z = M_0 - \gamma\hbar\textstyle\sum_k a_k^\dagger a_k \quad , \tag{6}$$

$$a_k = \lambda_k c_k - \mu_k c_{-k}^\dagger \quad , \tag{7}$$

$$c_k = \bar{c}_k e^{-i\omega t} \quad , \tag{8a}$$

$$c_{-k}^\dagger = \bar{c}_{-k}^\dagger e^{i\omega t} \quad , \tag{8b}$$

$$M_z(2\omega) = \gamma\hbar\textstyle\sum_k \lambda_k\mu_k \bar{c}_k^\dagger \bar{c}_{-k}^\dagger \quad . \tag{9}$$

In the above, M_z is the total z component of magnetization, $a_k^\dagger$ and a_k are the spin-deviation creation and annihilation operators, respectively, as defined by Holstein and Primakoff,[12] M_0 is the saturation magnetization at 0°K, and γ is the magnitude of the electronic-gyromagnetic ratio. The spin-deviation operators are related to the magnon operators c_k and $c_{-k}^\dagger$ by the Holstein-Primakoff transformation[12,13] whose parameters λ_k and μ_k are given by

$$\lambda_k^2 - |\mu_k|^2 = 1 \quad , \tag{10}$$

$$\lambda_k\mu_k = (\omega_M/4\omega_k)\sin^2\theta_k e^{-2i\phi_k} + B_a/2\omega_k \, , \tag{11a}$$

for $k \neq 0$,

and $$\lambda_0\mu_0 = B_a/2\omega_k \tag{11b}$$

for $k = 0$ and a sample with equal transverse demagnetizing factors. Here $\omega_M = 4\pi\gamma M_0$, θ_k and ϕ_k are polar and azimuthal angles, respectively, describing the direction of $\vec{k}$, and B_a is a contribution due to single-ion anisotropy. For cubic symmetry, $B_a = 0$ if the sample is magnetized along a $\langle 100\rangle$ or $\langle 111\rangle$ direction and $B_a = (3\gamma K_1/4M_0)$ if magnetized in a $\langle 110\rangle$ direction, where K_1 is the first-order cubic anisotropy constant. It is important to note that B_a is independent of $\vec{k}$ for single-ion anisotropy.

That spin-deviation and magnon operators are not one and the same, i.e., $\mu_k \neq 0$, results from terms in the dipolar and anisotropy Hamiltonians which do not commute with M_z. This also gives rise to time variation of M_z, expressed by $M_z(2\omega)$, which is that part of M_z which varies as $e^{2i\omega t}$. By referring to c_k and $c_k^\dagger$ as magnon operators, we mean that the part of the total Hamiltonian which is quadratic in the spin-deviation operators $\mathcal{H}^{(2)}$ may be reduced to

$$\mathcal{H}^{(2)} = \textstyle\sum_k \hbar\omega_k c_k^\dagger c_k \tag{12}$$

upon application of the Holstein-Primakoff transformation. It has been assumed in (8) that all excited spin waves are driven at the frequency ω. This implies resonance of the uniform mode under influence of a driving field at ω and excitation of spin waves by couplings such that $\omega_k = \omega_0$, as for the second-order Suhl process.

If the magnitudes and phases of the excited spin waves are independent of azimuthal angle ϕ_k and, as corresponds to our experiments, the sample has equal transverse demagnetizing factors and is magnetized in a direction such that $B_a \neq 0$, then the dipolar contribution to $\lambda_k\mu_k$ does not survive the summation in (9) and we are left with

$$M_z(2\omega) = \frac{\gamma\hbar B_a}{2\omega_k}\left(c_0^{\dagger 2} + \sum_{k\neq 0} \bar{c}_k^\dagger \bar{c}_{-k}^\dagger\right) \quad , \tag{13}$$

a form which will be assumed throughout.

In (13) the $k \neq 0$ and uniform-mode contributions have been separated for convenience. Suppose now that phase relations are assumed as in (5). Then (13) becomes

$$M_z(2\omega) = \frac{\gamma \hbar B_a}{2\omega_k} \bar{c}_0^{\dagger 2} \left[1 + i \sum_{k \neq 0} \left(\frac{g_{0k}^*}{\eta_k}\right) |c_k|^2\right] \quad . \quad (14)$$

Now[7] g_{0k} is real for all $\vec{k}$. It follows that the spin-wave contribution to second-harmonic power output, which is proportional to $|M_z(2\omega)|^2$, is simply additive.

Thus the assumption (5) of incoherent phase relations (as defined earlier) leads to a very definite prediction: The total second-harmonic power output $P_{2\omega}$ above threshold must be greater than or equal to that due to the uniform mode alone. Since the uniform-mode amplitude is found to increase above threshold, we may also state that $P_{2\omega}$ must increase above threshold. Our results show conclusively that this is *not* the case. $P_{2\omega}$ goes through a minimum above threshold, and at this minimum it is from 2 to 5 times less than $P_{2\omega}$ at threshold and from 12 to 30 times less than would be expected from the uniform mode contribution alone. (The varying numbers reflect differences in crystal orientation.)

Better accounting of the spin-wave phases is required to explain our results. Section IV gives a detailed treatment, but the qualitative features which provide agreement with experiment may be discussed here. Let $\vec{k}$ and $-\vec{k}$ be the first spin-wave pair to acquire large amplitude due to the Suhl process. When their amplitude becomes sufficiently large, they can excite another pair $\vec{k}'$, $-\vec{k}'$ by the same type parametric coupling. This is shown in Fig. 2. Assume for simplicity that $g_{0k'} = 0$ so that this new pair absorbs energy from the pair $\vec{k}$, $-\vec{k}$ alone. The phases $\bar{c}_0^2$, $\bar{c}_k \bar{c}_{-k}$, and $\bar{c}_{k'} \bar{c}_{-k'}$ are displayed in the diagram of Fig. 3. We have assumed $g_{kk'}$ and g_{0k} to be real and positive, which is the case for spin waves of interest.[14] The phase of $c_{k'}^{\dagger} c_{-k}^{\dagger}$ is given by an equation analogous to (5):

$$c_{k'}^{\dagger} c_{-k'}^{\dagger} = i(g_{kk'}/\eta_{k'}) c_k^{\dagger} c_{-k}^{\dagger} |c_{k'}|^2 \quad . \quad (15)$$

The important thing to observe in Fig. 3 is that $c_{k'} c_{-k'}$ is 180° out of phase with c_0^2 and thus, from (13), destructively interferes with the uniform mode's contribution to $P_{2\omega}$. In this way $P_{2\omega}$ can decrease above threshold for excitation of the second pair $\vec{k}'$, $-\vec{k}'$.

The fact that parametric processes occur between pairs of $k \neq 0$ spin waves as well as between a given $k \neq 0$ pair and the uniform mode has been ignored in the incoherent phase equation (3) which lumps all interactions not involving $k = 0$ into an effective relaxation rate and frequency shift. When the phase relations such as (15) demanded by parametric excitation are included it is possible to explain the striking harmonic generation effects to be described in Sec. III. These include sudden increase of $P_{2\omega}$ upon switching off the pulse of incident power and two or three peaks in the second-harmonic line profile, as well as the above-mentioned minimum in $P_{2\omega}$.

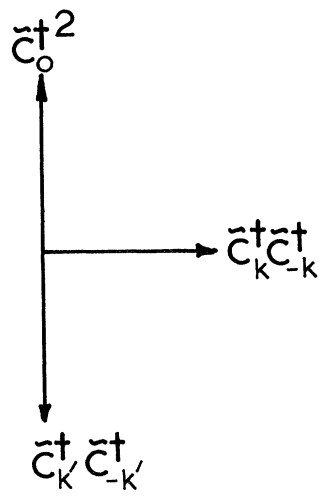

FIG. 3. Phasor diagram for uniform mode and excited spin waves. The pair $\vec{k}$, $-\vec{k}$ is excited by the process in Fig. 1(b), and the pair $\vec{k}'$, $-\vec{k}'$ by the process in Fig. 2. Coupling between $\vec{k}'$ and the uniform mode is neglected.

II. EXPERIMENTAL DETAILS

A. Samples

Experiments were performed at room temperature on highly polished single-crystal YIG spheres between 0.5 and 1.3 mm in diameter supplied by Airtron, Inc. These were found to have an intrinsic linewidth ΔH_0 of about 0.4 Oe at a fundamental frequency $\omega/2\pi = 8.42$ GHz. (ΔH_0 is the full width of the absorption curve at half-maximum in the limit of no radiation damping by the waveguide fields.) Detailed results to be presented here are for the largest, 1.3-mm-diam, sphere. Similar results were obtained for smaller samples although weaker-harmonic signals limited accuracy.

The sample was mounted on a quartz rod so that its ⟨111⟩ direction was approximately along the axis of the rod. This was accomplished by letting the sample rotate freely on a horizontal magnet pole face so that the easy ⟨111⟩ axis is vertical in equilibrium. It was then glued to a quartz rod with this position maintained. X-ray analysis later showed the sample to be orientated with its ⟨111⟩ direction

at an angle of $4^\circ \pm 3^\circ$ from the rod axis. With the rod perpendicular to the dc field $\vec{H}_0$, it was then possible by rotating the rod to vary approximately the direction of $\vec{H}_0$ in the (111) plane.

B. Microwave Circuitry

Power at the fundamental frequency $\omega/2\pi = 8.42$ GHz was furnished by a 20-W Varian VA-617G cw travelling wave tube (TWT). The TWT was driven by an X-13B reflex klystron whose output was modulated by a Philco diode switch. The diode was pulsed on by a Hewlett-Packard 212A pulser which has a rise time of 20 nsec. Because of the nonlinear character of the diode switch, the resulting pulses of microwave power had rise and fall times of 5 nsec.

A low-pass filter cut off at 12 GHz was placed in front of the TWT in order to prevent harmonics generated by the TWT from being detected.

The microwave circuit at the fundamental frequency is simply a shorted waveguide. But at the second-harmonic frequency it is a cavity resonant at $2\omega/2\pi = 16.84$ GHz with a loaded Q of about 2500. A cavity is not necessary at the fundamental because of the strength of the YIG transverse resonance. It is required at the second harmonic, though, in order to increase the level of radiated power to a conveniently detectable level. This circuitry is accomplished by the geometry shown in Fig. 4. X-band and $K\mu$-band waveguides are cross coupled by a circular iris. The $K\mu$-band guide acts as a short circuit to the fundamental fields while allowing second-harmonic energy to propagate through the iris. A reduced height section which is cut off to the TE_{01} mode below 22 GHz is placed at the input end of the X-band guide. The space between the reduced height section and the iris then forms a TE_{012} cavity which can be made to resonate at 2ω by proper adjustment of the sapphire tuning stub. The TE_{10} mode in which fundamental energy propagates is not significantly affected by the reduced height section [measured voltage standing-wave ratio (VSWR) was less than 1.1].

The sample is placed in the center of the cavity (which is $\frac{1}{2}\lambda_g$ from the effective short for the fundamental) as shown. In this position $M_z(2\omega)$ couples optimally to $h_z(2\omega)$ of the TE_{012} mode, and the uniform mode is excited by $h_x(\omega)$ of the TE_{10} mode.

C. Detection

Resonance at the fundamental frequency is detected by two methods. First, the standard technique of monitoring the reflected power is used. Second, the precessing transverse magnetization $M_\perp(\omega)$ is detected by a coupling loop in the x-z plane as shown in Fig. 4. The loop is particularly useful for transient measurements of the transverse magnetization since it responds only to fields generated by $M_\perp$. Steady-state measurements reported here were taken by the reflection method while transient data are from the loop.

The second-harmonic power on threshold radiated into the $K\mu$-band guide is of the order of 10^{-5} mW = -50 dBm (dB above 1 mW) for the cavity described above. This agrees well with the calculated value.[14] Since transient as well as steady-state measurements of $P_{2\omega}$ were performed, we had to balance sensitivity with bandwidth in designing a detection scheme. The most satisfactory arrangement with available equipment proved to be superheterodyne detection and video amplification

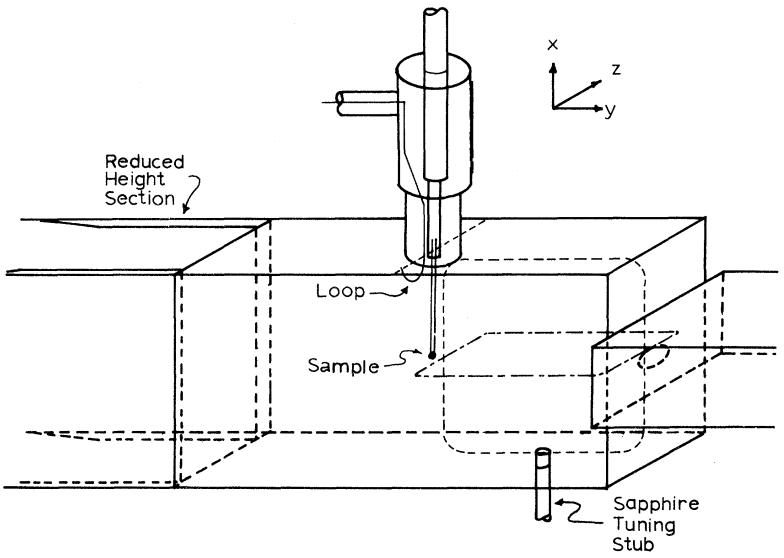

FIG. 4. Second-harmonic cavity and details of sample position, rf fields, waveguide coupling, and coupling loop for detection of transverse magnetization. The dotted line indicates the fundamental h fields and the dot-dashed line indicates second-harmonic h fields.

for most of the measurements. An X-12 klystron was used as a local oscillator, and the i.f. frequency was 80 MHz. The i.f. envelope was amplified with a Hewlett-Packard 462A video amplifier and displayed directly on the face of a Tektronix 581A oscilloscope. In this way powers of − 60 dBm could be detected. Straight video detection could be used at higher powers where sensitivity was not an overriding factor.

The cavity Q limited the response time to 50 nsec. For some measurements it was necessary to look at shorter-time responses. Here we removed the iris, thereby reducing the loaded Q to about 300 and cavity ring time to about 5 nsec. (A cavity remained at 2ω because of the discontinuity between X- and $K\mu$-band guides.)

D. Measurement of Second-Harmonic Phase

Phase of the second-harmonic signal was measured by the following method, shown in Fig. 5. Some (− 20 dB) of the incident fundamental power is fed into a crystal diode which is used as a harmonic generator. The second harmonic produced in this way has a constant phase with respect to the incident fields at ω and hence with respect to the uniform mode if resonance conditions are maintained. It is then mixed with the second harmonic generated from the sample. One can measure how the phase of the 2ω signal generated from the sample varies with power by observing the amount of phase shift which has to be introduced by the precision phase shifter in order to minimize the detected signal. He must, of course, not make any adjustments of attenuators beyond the coupler in Fig. 5, nor do anything else to introduce an extra phase shift as the power is increased. Also, the phase difference between ω incident upon and 2ω generated from the diode must not depend on power level. This was checked and found to be the case.

E. Coupling of Sample to Waveguide Fields

Parameters are measured as a function of rf driving field h at the fundamental frequency. As used throughout, h is the field which exists in the sample. It is related to h_0, the waveguide field in the absence of the sample, on magnetic resonance by[4,14]

$$h = h_0/(1+\beta) \quad , \tag{16}$$

where β is the sample coupling coefficient

$$\beta = 16\pi^2 V_s \chi''/\lambda_g ab \tag{17}$$

for the sample located as in Fig. 4 where V_s is the sample volume, λ_g is the guide wavelength, ab is the waveguide cross section, and χ'' is the imaginary part of the rf susceptibility on resonance.

Experimentally, β is measured as

$$\begin{aligned} \beta &= r \ , \quad \text{overcoupled sample} \\ &= 1/r, \quad \text{undercoupled sample,} \end{aligned} \tag{18}$$

where r is the VSWR on resonance, it being assumed the fundamental frequency microwave circuit is a shorted waveguide so that $r \to \infty$ well off resonance. Distinction between overcoupled and undercoupled can readily be made by microwave techniques.[15]

The 1.3-mm-diam sphere was overcoupled with $\beta = 9$. Such strong coupling, even without a cavity, is typical for YIG. The large value of β has two important consequences. First, h^2 is not proportional to incident power above threshold since χ'' is power dependent in this region. Second, there is a sizable radiation-damping contribution to linewidth. Analysis[14] shows that

$$\Delta H_L = \Delta H_R + \Delta H_0 = \Delta H_0(1+\beta) \quad , \tag{19}$$

where ΔH_L, the loaded linewidth, is what is observed experimentally, ΔH_R is the radiation damping contribution to linewidth, and ΔH_0 is the previously defined intrinsic linewidth. From measurement of ΔH_L and VSWR on resonance, (18) and (19) can be used to determine ΔH_0.

Transient decay of the uniform mode occurs at a rate $\gamma \Delta H_L$ which, for the 1.3-mm sample, is 10 times faster than the intrinsic decay rate $\gamma \Delta H_0$. Spin waves decay at their intrinsic rates, however, since $k \neq 0$ modes do not couple to transverse driving fields. This feature enables us to study the $k \neq 0$ contribution to second harmonic by observing the decay rate of $M_z(2\omega)$, since for times much greater than $(\gamma \Delta H_L)^{-1}$ it is dominated by $k \neq 0$ spin waves.

Coupling of $M_z(2\omega)$ to the second-harmonic cav-

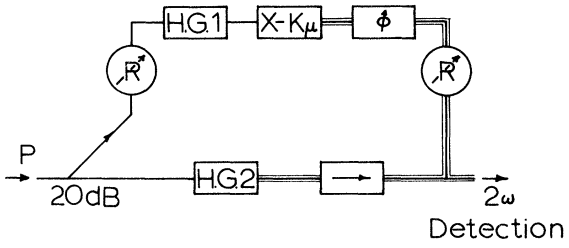

FIG. 5. Microwave circuitry for measurement of second-harmonic phase. The solid lines indicate the X-band waveguide and the thick and thin lines, the $K\mu$-band waveguide; R is the variable attenuator; the arrow is the isolator; the circle with an arrow is precision phase shifter; X-$K\mu$ is the X-band to $K\mu$-band transition; H. G. 1 is the diode harmonic generator; H. G. 2 is the YIG sample harmonic generator; 20 dB is the 20-dB directional coupler. X-band components related to coupling fundamental power P_{in} into sample and detection of reflected power are not shown.

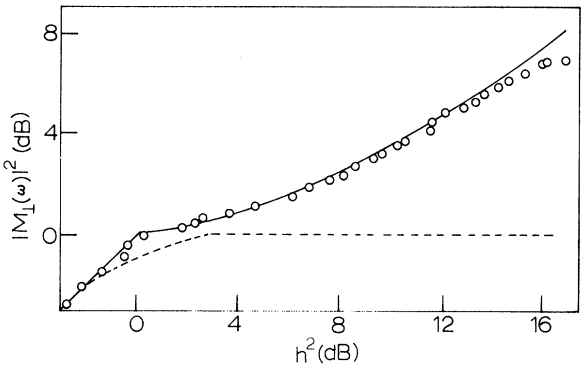

FIG. 6. Square of transverse magnetization $|M_\perp(\omega)|^2$ versus square of driving field at sample h^2. Suhl threshold occurs at 0 dB, which corresponds to $h = 6.5\times10^{-3}$ Oe. The solid curve is Eq. (30) with $C' = \frac{1}{2}$. The dashed curve shows behavior for inhomogeneity scattering.

ity fields can, in principle, lead to radiation damping of the uniform and $k \neq 0$ modes. But for the low efficiency of harmonic generation reported here, this effect is completely negligible.

III. RESULTS

A. Uniform-Mode Resonance

Figure 6 shows transverse magnetization $|M_\perp(\omega)|$ versus fundamental rf field h. Threshold is clearly recognized, as is the fact that $|M_\perp(\omega)|$ increases above threshold. The critical field is $h_c = 6.5\times10^{-3}$ Oe, and the intrinsic linewidth is $\Delta H_0 = 0.38$ Oe. From the relation[1,7]

$$h_c = \Delta H_0(\Delta H_k/4\pi M)^{1/2}, \qquad (20)$$

we obtain $\Delta H_k = 0.51$ Oe as the full linewidth of the z-directed spin wave, which is the first to go unstable since it has the maximum coupling g_{0k}. In (20), $4\pi M = 1750$ G is the saturation magnetization of YIG at room temperature.

Above threshold the dc field H, required for resonance, changes with power level, as observed by Matcovich *et al.*[16] Data were taken with H adjusted to give resonance at each power level. The solid curve in Fig. 6 is theoretical and is discussed in Sec. IV A. The dashed curve shows the expected behavior when two magnon-scattering processes are included[6] but nonlinear processes between $k \neq 0$ spin waves are ignored. Both the general shape of the curve above threshold and the value of ΔH_k agree closely with previous measurements.[5] Linewidths and behavior of $|M_\perp(\omega)|$ above threshold are insensitive to orientation of $\vec{H}$ in the (111) plane, although the value of H required for resonance does vary in a manner well correlated[14] with theory.

Relaxation oscillations[17] occur for h^2 greater than 16 dB above threshold and prevent meaningful measurements from being taken.

B. Second-Harmonic Power Output

Second-harmonic power output $P_{2\omega}$ is shown as a function of h in Fig. 7 for three different orientations of $\vec{H}$ approximately in the (111) plane. Powers are normalized to the values at threshold. Below threshold the absolute value of $P_{2\omega}$ varies with angle in a manner which agrees with the theoretical variation of B_a (13) in the (111) plane.[14] This is such that $P_{2\omega}$ is a maximum with $\vec{H}$ in the [110] direction and is a minimum with $\vec{H}$ at an angle of 30° with respect to [110]. The ratio between maximum and minimum $P_{2\omega}$ is about 9.

The dashed curve represents the expected $P_{2\omega}$

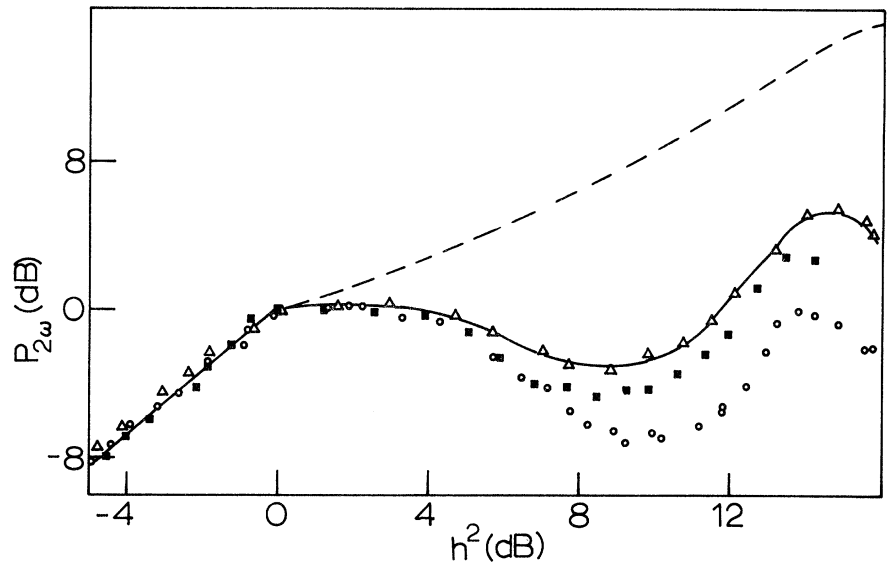

FIG. 7. Normalized second-harmonic power output versus square of driving field. 0 dB corresponds to threshold. The circles indicate $\vec{H}$ along [110]; the squares, $\vec{H}$ 10° from [110] approximately in (111) plane; the triangles, $\vec{H}$ 20° from [110] approximately in (111) plane. The dashed curve is $P_{2\omega} \propto |M_\perp \times (\omega)|^4$ which represents contribution from uniform mode alone. The solid curve through Δ data is Eq. (42) with α and ν given by Fig. 11.

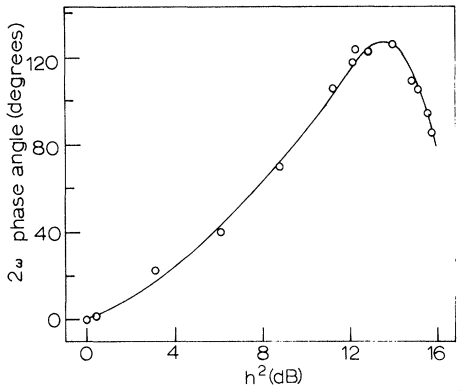

FIG. 8. Phase of second harmonic versus square of driving field. Data are for $\vec{H}$ 20° from [110] approximately in (111) plane, corresponding to Δ points of Fig. 7. The solid curve is obtained from Eq. (42) with α and ν given by Fig. 11.

due to the uniform mode alone. This is given by

$$P_{2\omega}(k=0) \propto |\tilde{c}_0^4| \propto |M_\perp(\omega)|^4 \quad ,$$

as follows from (13). Above threshold, the total $P_{2\omega}$ is considerably less than the $k=0$ contribution, in marked disagreement with the picture (5), (15) in which all excited spin waves have phases such that they absorb power directly from the uniform mode.

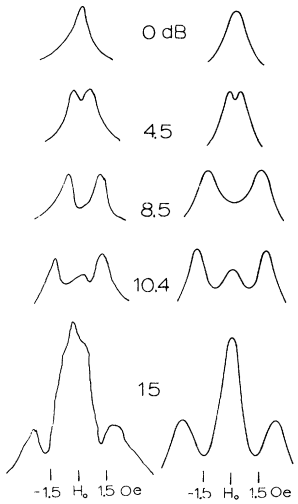

FIG. 9. Second-harmonic power versus dc field H. Orientation of H is the same as for Δ points of Fig. 7. Numbers in dB refer to the level of h^2 above threshold. Curves on the left are experimental. Curves on the right are theoretical as explained in Sec. IV C. Transverse magnetization gives a single resonance line at all power levels centered at H_0. (The value of H_0 does change with power level, and the width of the resonance curve increases with power.)

C. Second-Harmonic Phase

Phase of the second harmonic $M_z(2\omega)$ is shown in Fig. 8 for one crystal orientation. If we let

$$M_z(2\omega) = \tilde{c}_0^{\dagger 2} F(2\omega) \quad , \tag{21}$$

then the phase angle Φ_s is given by

$$\tan\Phi_s = \mathrm{Im}F(2\omega)/\mathrm{Re}F(2\omega) \quad , \tag{22}$$

where Im and Re stand for imaginary and real parts, respectively. Since the dc field is adjusted to keep the uniform mode on resonance, the phase of $\tilde{c}_0^\dagger$ is constant with respect to the incident driving field. This, together with the fact that the phase of the second-harmonic cavity field is constant with respect to $M_z(2\omega)$, enables Φ_s to be measured by the method discussed in Sec. II C.

Note that Φ_s exceeds 90° for a range of powers above threshold. This is incompatible with Eq. (15) if

$$\sum_{k\neq 0} (g_{0k}^*/\eta_k)|c_k|^2 > 0 \, .$$

Examination of g_{0k} shows that this certainly should be the case[7] since $|g_{0k}|$ is very small for $g_{0k}<0$ and thus there should be relatively few spin waves excited with $g_{0k}<0$. Hence both the phase-shift and $P_{2\omega}$ data refute the predictions based on incoherent phase relations among $k\neq 0$ spin waves.

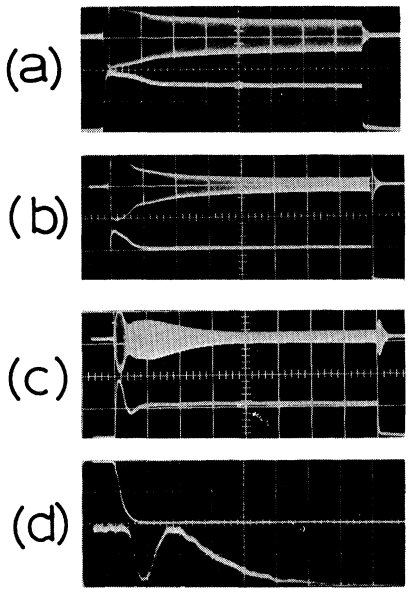

FIG. 10. Second-harmonic and transverse magnetization pulse shapes (a) 6 dB above threshold, 1 μsec/cm; (b) 9.6 dB above threshold, 1 μsec/cm; (c) 14 dB above threshold, 1 μsec/cm; (d) 8 dB above threshold, 50 nsec/cm. In (a)–(c) the upper trace is second-harmonic (if envelope) and the lower trace transverse magnetization. In (d) the lower trace is second-harmonic (straight video detection) and the upper trace transverse magnetization.

The solid curve in Fig. 8 is theoretical and is explained in Sec. IV B.

D. Second-Harmonic Line Profile

Dependence of $P_{2\omega}$ upon applied field H has particularly interesting features as seen in Fig. 9. Below threshold, a single peak appears at the field required for resonance H_0. In the region between threshold and the minimum in $P_{2\omega}$, two peaks are seen with a minimum occurring at H_0. As h is increased above the point where $P_{2\omega}$ has a minimum, three peaks appear with the one at H_0 growing relative to the other two. Over the whole range, however, the uniform-mode resonance gives only a single line. Theoretical curves are shown alongside the experimental ones. These are discussed in Sec. IV C.

E. Pulse Shapes

In Fig. 10 we present a series of fundamental and second-harmonic pulse shapes observed between 6 and 14 dB above threshold for $\vec{H}_0$ along $\langle 110 \rangle$. Other crystal orientations give similar results. Below threshold the pulse shapes are essentially square on the 1-μsec/cm scale. The fundamental pulses record $|M_\perp(\omega)|^2$ as detected with the pickup loop (Sec. II C).

The transverse magnetization has an initial spike above threshold, but no other unusual features. The second-harmonic pulse, however, has additional peculiarities besides the initial spike. For h^2 greater than about 10 dB above threshold, $P_{2\omega}$ shows an initial increase after the pulse of incident power is turned off. At about 12 dB above threshold $P_{2\omega}$ develops a second peak after the initial spike. Results quoted in Secs. II B and II D referred to the steady-state portion of the $P_{2\omega}$ pulse after the second peak has decayed out.

The traces in Figs. 10(a)–10(c) were taken with $Q_L = 2500$ for the loaded Q of the second-harmonic cavity. In Fig. 10(d) the loaded Q was reduced to about 300 so that the initial decline in $P_{2\omega}$ could be observed. This effect is masked with the larger Q since it occurs in a time shorter than the response time for $Q_L = 2500$.

Theoretical curves are presented in Sec. IV D which reproduce qualitative aspects of those shown here.

F. Relaxation Rate of Spin Waves from $P_{2\omega}$

Since the uniform mode decays very rapidly (decay time $\approx$ 15 nsec) because of radiation damping the long-time trailing edge of the $P_{2\omega}$ pulse is assumed to be due to $k \neq 0$ spin waves. Its long-time decay constant gives a measure of the relaxation rate of spin waves which contribute to second harmonic. We find this rate corresponds to $\Delta H_k = 0.63$ Oe approximately independent of power level for h^2 greater than 9.6 dB above threshold. At lower powers, the signals were too weak for meaningful measurement to be performed. This value of ΔH_k is close to the figure 0.51 Oe obtained from the critical rf field (Sec. III A).

Time bases as shown in Fig. 10(d) were used for these measurements.

IV. THEORY AND INTERPRETATION OF RESULTS

We show in this section that the peculiarities associated with second-harmonic generation can be explained at least qualitatively by accounting for parametric coupling among $k \neq 0$ spin waves and the ensuing phase relations. The behavior of transverse magnetization above threshold can, however, be reproduced by a simpler effective-relaxation-rate theory, which is demonstrated in Sec. IV A.

A. Uniform Mode above Threshold

Above threshold the uniform mode couples directly to a pair of z-directed spin waves $\vec{k}$ and $-\vec{k}$. Following Schlömann's treatment[9] of parallel pumping[18,19] above threshold, we assume that as the amplitudes of $\vec{k}$ and $-\vec{k}$ grow their relaxation rate η_k increases. This is caused by nonlinear processes involving destruction of magnons $\vec{k}$ and $-\vec{k}$. If the net effect of these simply is to make η_k power dependent then (4) still holds but with η_k not a constant. Schlömann took

$$\eta_k = \eta_k(0)(1 + \Delta T/T) \quad , \tag{23}$$

where $\eta_k(0)$ is the spin-wave relaxation rate below threshold, T is the lattice and spin-wave temperature below threshold, and ΔT the increase in temperature of the spin waves above threshold. The increase in spin-wave temperature ΔT is assumed to be proportional to P_k, the energy absorbed per sec by the spin waves:

$$\Delta T/T = CP_k \quad , \tag{24}$$

where C is an appropriate constant. Now P_k is given from conservation of energy considerations by

$$P_k = P - P_0 \quad , \tag{25}$$

where P is the total power dissipated by the system of spin waves plus uniform mode and P_0 is the power dissipated by the uniform mode. We have

$$P = \tfrac{1}{2}\omega\chi''h^2 \propto |c_0|h \tag{26}$$

and

$$P_0 = 2\eta_0\hbar\omega_0|c_0|^2 \quad . \tag{27}$$

Equation (26) expresses the fact that the total energy absorbed from the driving field arises from

coupling of the uniform mode to h since the $k \neq 0$ modes do not couple directly. In the steady state, the total energy absorbed is, of course, equal to the total energy dissipated.

It is convenient to introduce normalized variables defined by

$$x = h/h_{\text{crit}} \quad , \tag{28a}$$

$$y = |c_0|/|c_0|_{\text{crit}} \quad , \tag{28b}$$

so that x and y represent, respectively, rf field and uniform-mode amplitudes normalized to their values on threshold. Then (24) becomes, with use of (25)–(27),

$$\Delta T/T = C'y(x-y) \quad , \tag{29}$$

where C' is a new constant. With (29) in (23) and (4) we then have

$$y^2 = 1 + C'y(x-y) \tag{30}$$

for the predicted dependence of uniform-mode amplitude on rf field (y versus x) above threshold. Equation (30) with $C' = \frac{1}{2}$ is shown as the solid line in Fig. 6. It is seen that the power-dependent relaxation-rate method of Schlomänn gives a good description up to 12 dB above threshold.

We note that the measured value $\Delta H_k = 2\eta_k/\gamma = 0.51$ Oe (Sec. III A) is in exact agreement with the theory of Sparks, Loudon, and Kittel[20] for relaxation of a z-directed spin wave by the three-magnon confluence process. This strengthens our basic premise that the initial departure from linearity in Fig. 6 is due to the second-order Suhl threshold for a homogeneous specimen, and not caused by inhomogeneity scattering which leads to a gradual decrease in susceptibility for $|c_0|^2 < \eta_k/g_{0k}$.

B. Second Harmonic, Power Output, and Phase

As mentioned previously, the simple phase relation (5) is totally inadequate for explaining second-harmonic data. Before proceeding to analyze phase relations in the presence of parametric coupling between $k \neq 0$ spin waves, we wish to justify an assumption used throughout: The excited spin waves all have effective frequency $\tilde{\omega}_k = \tilde{\omega}_0 = \omega$. It is important that this be examined since if the spin waves are not excited in resonance ($\tilde{\omega}_k \neq \tilde{\omega}_0$), then one can expect departures from (5) even for a single pair of excited magnons. The second equality, $\tilde{\omega}_0 = \omega$, is always satisfied by proper adjustment of H to ensure resonance of the uniform mode. The symbols $\tilde{\omega}_k$ and $\tilde{\omega}_0$ are used to account for power-dependent frequency shifts.

To discuss the above question we replace the term $\eta_k c_k$ by $\eta_k(c_k - \bar{c}_k)$ in (3) where $\bar{c}_k$ is the thermal equilibrium value of c_k. This allows c_k to have a finite value below threshold. Solutions of (3) and a similar equation for $\dot{c}_{-k}^{\dagger}$ then give for an $e^{i\tilde{\omega}_0 t}$ time dependence

$$c_k^{\dagger} c_{-k}^{\dagger} = \frac{2i\,|\bar{c}_k|^2 \eta_k^2 g_{0k}^* c_0^{\dagger 2}\{\eta_k + i(\tilde{\omega}_k - \tilde{\omega}_0)\}}{[(\tilde{\omega}_k - \tilde{\omega}_0)^2 + \bar{\eta}_k^2]^2} \quad , \tag{31}$$

where random phases of $\bar{c}_k$ and $\bar{c}_{-k}$ have been assumed and where

$$\bar{\eta}_k^2 = \eta_k^2 - |g_{0k}|^2 |c_0|^4 \quad . \tag{32}$$

The first term in curly brackets of (31) leads to the phase relation (5). The term $i(\tilde{\omega}_k - \tilde{\omega}_0)$ causes a departure from (5), but it is negligible for the following reasons. From the denominator in (31) we see that $c_k^{\dagger} c_{-k}^{\dagger}$ is appreciable only for $|\tilde{\omega}_k - \tilde{\omega}_0| \lesssim \bar{\eta}_k$. Thus the ratio of the second to the first term in curly brackets of (31) should not be greater than the order of $\bar{\eta}_k/\eta_k$. But for spin waves excited to large amplitude by parametric coupling, $\bar{\eta}_k \to 0$, and thus $\bar{\eta}_k \ll \eta_k$ for the important spin waves. The same point has been made by Schlömann[21] in showing that $\bar{\eta}_k$ is sufficiently small that effects may be observed due to discreteness of the spin-wave spectrum. A second reason for ignoring the $\tilde{\omega}_k - \tilde{\omega}_0$ contribution to phase shift is that if a group of spin waves centered about $\tilde{\omega}_k = \tilde{\omega}_0$ is excited then the summation $\sum_k c_k^{\dagger} c_{-k}^{\dagger}$ is involved. The magnitudes of the contributions of the η_k and $\tilde{\omega}_k - \tilde{\omega}_0$ terms in curly brackets of (31) will then have a ratio of the order of $g_{0k}/\bar{\eta}_k(\partial g_{0k}/\partial \omega_k)$, which should be of the order of $\omega_k/\bar{\eta}_k \gg 1$.

Having seen that nonresonant ($\tilde{\omega}_k \neq \tilde{\omega}_0$) excitation of spin waves cannot account for significant departures from the simple phase relation (5), we now examine parametric processes involving $k \neq 0$ spin waves. The other terms in (1) are written so as to take explicit account of four-magnon processes in which $\vec{k}$ and $-\vec{k}$ are converted to $\vec{k}'$ and $-\vec{k}'$ (Fig. 2). All other scattering processes are assumed to be describable by effective relaxation rates and frequency shifts. Thus (3) becomes

$$\dot{c}_k = -i\tilde{\omega}_k c_k - \eta_k c_k - i g_{0k} c_0^2 c_{-k}^{\dagger} - i \sum_{k' \neq 0} g_{kk'} c_{k'} c_{-k'} c_{-k}^{\dagger} \quad , \tag{33}$$

where $g_{kk'}$ is the coupling constant appropriate to the four-magnon process in Fig. 2, and $g_{kk} = 0$. Since only a portion of the scattering terms has been treated explicitly, (33) is still not exact, but it should contain the most important parametric terms. The reasons for sorting out the $\vec{k}$, $-\vec{k} \to \vec{k}'$, $-\vec{k}'$ terms as opposed to three-magnon or $\vec{k}$, $\vec{q} \to \vec{k}'$, $-\vec{k}' + \vec{k} + \vec{q}(\vec{q} \neq -\vec{k})$ processes are that (a) only processes of this type give rise to a coherent phase between spin waves $\vec{k}'$ and $-\vec{k}'$, and such phase coherence is necessary in order for the pair

to contribute to $P_{2\omega}$ (13). That is, if $\vec{k}'$ is excited by one scattering and $-\vec{k}'$ by another, they will not – at least in first approximation – contribute to second harmonic since their phases will be random; (b) the initial spin waves to have large amplitude are of opposite momenta since they are excited from the uniform mode. The next energy- and momentum-conserving nonlinear process which can then occur is one in which the initial pair scatters into another pair since relatively large amplitudes of the incident magnons are required. A three-magnon splitting process $\vec{k} \rightarrow \vec{k}'$, $\vec{k} - \vec{k}'$ is not allowed since we assume that the first-order Suhl process is forbidden, and thus there are no spin waves $\vec{k}'$ for which $\tilde{\omega}_{k'} = \frac{1}{2}\omega_0 = \frac{1}{2}\omega_k$. Thus (33) does account for the initial parametric processes properly.

We assume an $e^{i\tilde{\omega}_0 t}$ time dependence and $\tilde{\omega}_k = \tilde{\omega}_0$ for all spin waves, as discussed previously. Steady-state solution to (33) then yields, similar to (5),

$$c_k^\dagger c_{-k}^\dagger = i\left(\frac{g_{0k}^*}{\eta_k} c_0^{\dagger 2} + \sum_{k' \neq 0} g_{kk'}^* c_{k'}^\dagger c_{-k'}^\dagger\right) |c_k|^2 \quad . \tag{34}$$

If a phase angle Φ_k is defined by

$$c_k^\dagger c_{-k}^\dagger = i\,|c_k|^2 c_0^{\dagger 2} e^{i\Phi_k}/|c_0|^2 \quad , \tag{35}$$

then (34) becomes

$$e^{i\Phi_k} = \frac{g_{0k}^*}{\eta_k}|c_0|^2 + \frac{i}{\eta_k}\sum_{k' \neq 0} g_{kk'}^* |c_{k'}|^2 e^{i\Phi_{k'}} \quad . \tag{36}$$

The relation (13) for $M_z(2\omega)$ is

$$M_z(2\omega) = \frac{\gamma\hbar B_a}{2\omega_k}\tilde{c}_0^{\dagger 2}\left(1 + i\sum_{k \neq 0}\frac{|c_k|^2 e^{i\Phi_k}}{|c_0|^2}\right). \tag{37}$$

Thus an expression is needed for $|c_k|^2 e^{i\Phi_k}$ summed over the excited spin waves. For the sake of obtaining a solution we assume that $\sum_{k' \neq 0} g_{kk'}^* |c_{k'}|^2/\eta_{k'}$ is independent of $\vec{k}$. This can be reasonable well above threshold when many spin waves should be excited. However, it is of questionable validity immediately above threshold where only one spin-wave pair has large amplitude. With this assumption (36) then gives

$$\sum_{k \neq 0}|c_k|^2 e^{i\Phi_k} = \sum_{k' \neq 0}\frac{g_{0k'}}{\eta_{k'}}|c_{k'}|^2 |c_0|^2 \times\left(1 - i\sum_{k' \neq 0}\frac{g_{kk'}^*}{\eta_{k'}}|c_{k'}|^2\right)^{-1} . \tag{38}$$

The above shows that as the number of excited spin waves increases the net phase of the spin waves with respect to the uniform mode is such as to introduce a component which interferes destructively with $\tilde{c}_0^{\dagger 2}$ in the contribution to $P_{2\omega}$ (for $g_{kk'}^*$ and g_{0k}^* of the same sign). This confirms the physical picture discussed in connection with Fig. 3.

The next step is to obtain an expression for $\sum_{k \neq 0}|c_k|^2$. The groundwork for this has been laid in Eqs. (25)–(27), which give power absorbed and dissipated by the $k \neq 0$ spin waves and the uniform mode. Since we assume $\omega_k = \omega_0$ for all excited spin waves, the expression for the spin-wave energy dissipated per sec is, analogous to (27),

$$P_k = 2\hbar\omega_0 \sum_{k \neq 0}\eta_k |c_k|^2 \quad . \tag{39}$$

Use of (26), (27), and (39) then gives

$$\sum_{k \neq 0}|c_k|^2 = \frac{\eta_0}{\langle\eta_k\rangle}|c_0|^2_{\text{crit}}\, y(x-y) \tag{40}$$

in terms of the normalized variables x and y (28). The quantity $\langle\eta_k\rangle$ represents an average of η_k over the excited spin waves:

$$\langle\eta_k\rangle = \sum_{k \neq 0}\eta_k |c_k|^2 / \sum_{k \neq 0}|c_k|^2 \quad . \tag{41}$$

With (40) and (38) in (37), we then get

$$M_z(2\omega) \propto y^2\left[1 - \frac{\alpha\nu y^2(x-y)^2}{1+\alpha^2 y^2(x-y)^2} + i\,\frac{\nu y(x-y)}{1+\alpha^2 y^2(x-y)^2}\right], \tag{42}$$

where $$\alpha = \langle g_{kk'}^*/\eta_k\rangle(\eta_0/\langle\eta_k\rangle)\,|c_0|^2_{\text{crit}} \quad , \tag{43a}$$

$$\nu = \langle g_{0k}/\eta_k\rangle(\eta_0/\langle\eta_k\rangle)\,|c_0|^2_{\text{crit}} \quad , \tag{43b}$$

with averages $\langle\,\rangle$ defined as in (41) with respect to the distribution of excited spin waves.

The effect of coupling between $k \neq 0$ spin waves, expressed by α, is seen to reduce $|M_z(2\omega)|$ both by adding a component 180° out of phase with $c_0^{\dagger 2}$ [second term in (42)] and by reducing the 90° component [third term in (42)]. With $\alpha = 0$ (42) reduces to (14).

The second-harmonic phase Φ_s (22) has its tangent given by the ratio of the imaginary to the real parts of the expression in brackets of (42). For $\nu > \alpha$, it is possible to have $\Phi_s > 90°$ sufficiently far above threshold, in agreement with experiment (Fig. 8).

Equation (42) has been compared with experiment by treating α and ν as adjustable parameters which are uniquely determined by $P_{2\omega}$ and Φ_s. The quantities x and y are taken from the data of Fig. 6. It is reasonable to expect α and ν to decrease

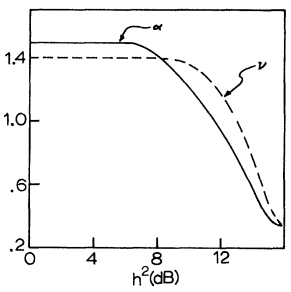

FIG. 11. Dependence of parameters α and ν [Eq. (43)] upon square of driving field. Solid curves of Figs. 7 and 8 are obtained from this figure and Eq. (42).

with increasing power well above threshold. This is because η_k must be regarded as an effective relaxation rate into which all nonlinear processes other than the $\vec{k}$, $-\vec{k}\rightarrow\vec{k}'$, $-\vec{k}'$ ones are lumped. Also $\langle g_{0k}/\eta_k\rangle$ can be expected to decrease even for constant η_k as spin waves are excited which couple more weakly to the uniform mode than the initial pair. Thus we have attempted to fit the data of Figs. 7 and 8 (20° orientation only for Fig. 7) with values of α and ν which are not allowed to increase with h. The resulting α and ν are shown in Fig. 11, and the theoretical curves are the solid ones in Figs. 7 and 8. Above the region where α and ν are constant, the points in Fig. 11 correspond to the values required to obtain exact agreement. At lower powers ν must increase with h in order to get perfect agreement. Use of a constant in this range has a negligible effect on $P_{2\omega}$, but does produce as much as 20% error in Φ_s, as seen. It is noteworthy that with α and ν decreasing functions of h it is possible to describe the maximum in $P_{2\omega}$ at about 15 dB above threshold.

The values of α and ν used in the constant region of Fig. 11 are 1.5 and 1.4, respectively. They can be estimated theoretically from the experimental measurements of ΔH_k and ΔH_0. Since $\eta_k/g_{0k} = |c_0|^2_{\rm crit}$ on threshold, we should have $\nu=\eta_0/\eta_k = 0.75$. The quantity $g_{kk'}$ is[14] approximately equal to g_{0k} for $\vec{k}$ and z-directed spin wave, so we should expect $\alpha\approx\nu$. Hence there is about a factor of 2 discrepancy between the predicted α and ν and the ones given in Fig. 8. This, together with the fact that ν must increase initially in order to reproduce the phase shift, is perhaps indicative of the weakness of our assumptions immediately above threshold, as discussed prior to Eq. (38). We also point out, though, that since (21) $\Delta H_k/\Delta H_0$ is proportional to $h_c^2/\Delta H_0^3$, 10% errors in the measurement of ΔH_0 and h_c could alter the ratio $\Delta H_k/\Delta H_0$ by a factor of 1.7, so the factor of 2 error in α and ν may not be too serious.

Equation (42) differs slightly from a previous version.[22] In the earlier work we treated Φ_k as independent of $\vec{k}$ and solved (36) for $\tan\Phi_k$. This leads to an inconsistency which was not appreciated at the time. Phase-shift measurements had not yet been performed then, so the unique determination of α and ν was not possible.

C. Second-Harmonic Line Profile

The structured $P_{2\omega}$ line shapes of Fig. 9 may be understood in terms of the dependence of $P_{2\omega}$ versus h on resonance (Fig. 7). To do this we make the following assumption: The power output at any dc field H depends only on the uniform-mode amplitude. That is, for a given value of $|c_0|^2$, $P_{2\omega}$ is the same whether this value is attained on resonance ($H=H_0$) or off resonance ($H\neq H_0$). Justifications for this assumption are that (a) the ellipticity of the modes, which gives rise to second harmonic, is independent of $H-H_0$ because it is governed by the natural elliptical precession of the mode ($\lambda_0\mu_0\neq 0$). A case for which ellipticity does depend on $H-H_0$ occurs for $\lambda_0\mu_0=0$. Then the natural precession is circular, and second-harmonic generation is possible only by excitation of both the ressonant and counter-rotating senses of circular polarization. As long as $\lambda_0\mu_0 \gg \Delta H_0/H_0$, effects of the counter-rotating component on $P_{2\omega}$ may be neglected. For YIG with $\vec{H}$ in the (111) plane, this condition is well satisfied. (b) Nonlinear excitation of spin waves takes place by coupling to the uniform mode rather than the driving field. Thus, for example, Eq. (33) involves only c_0^2, and no mention need be made of whether or not the uniform mode is on resonance.

Consider then one of the curves in Fig. 7, which gives $P_{2\omega}$ versus h^2 for H adjusted to resonance. This can readily be converted to $P_{2\omega}$ versus y^2 (28a) by use of Fig. 6. The general shape of $P_{2\omega}$ versus y^2 is the same as $P_{2\omega}$ versus h^2 since y is an increasing function of h. Now as H is varied off resonance y decreases. To be specific, we take a Lorentzian

$$y^2 = y_0^2[1+4(H-H_0)^2/\Delta H_L^2]^{-1} \quad , \tag{44}$$

where y_0 is the value of y on resonance. The loaded linewidth ΔH_L is used since H is varied at constant driving field h_0 (see Sec. II E.). As y decreases from y_0 to zero, $P_{2\omega}$ then assumes in succession all values on the curve $P_{2\omega}$ versus y^2 for $y\leq y_0$. Thus, for example, if we are at the minimum in $P_{2\omega}$ (about 10 dB above threshold) with H on resonance, then as H is moved off resonance $P_{2\omega}$ increases since decrease in y means an increase in $P_{2\omega}$ in this region. A maximum in $P_{2\omega}$ versus H occurs for $y\approx 1$ as can be seen from Fig. 7. Also it is evident that for h^2 above the value at the minimum in $P_{2\omega}$, there will be a local maximum in $P_{2\omega}$ on resonance while for h^2 less than that required for the minimum, $P_{2\omega}$ will go through a minimum on resonance.

Quantitative line shapes $P_{2\omega}(H)$ are readily obtained from Figs. 6 and 7 and Eq. (44). Thus we have

$$P_{2\omega}(H) = P_{2\omega}\{x[y(H)]\} \quad , \tag{45}$$

indicating that $P_{2\omega}$ is a function of driving field x (28a) which is a function of uniform-mode amplitude y which is in turn a function of dc field H. The resulting curves in Fig. 9 are seen to agree well with experiment.

D. Pulse Shapes

1. *Transient Decay*

Keys to behavior of the second-harmonic pulse after the incident fundamental power has been turned off are the vector diagrams of Fig. 12 and the fact that the uniform mode decays much more rapidly than the $k \neq 0$ spin waves due to radiation damping. The spin-wave contribution to $P_{2\omega}$, $\sum_k \times \tilde{c}_k^{\dagger} \tilde{c}_{-k}^{\dagger}$ is divided into components 90° and 180° out of phase with $\tilde{c}_0^{\dagger 2}$. Figure 12(a) is for the 180° component k_{180} less than $|c_0|^2$ in the steady state. In this case, $|M_z(2\omega)|$ decreases during the rapid decay of the uniform mode, as long as $|c_0|^2 > k_{180}$. After $|c_0|^2$ has decayed to the level k_{180}, $|M_z(2\omega)|$ increases until such time as relaxation of the k_{90} and k_{180} components becomes important. This situation corresponds to the trace in Fig. 10(d).

Figure 12(b) is for k_{180} greater than $|c_0|^2$ in the steady state. Then $|M_z(2\omega)|$ initially increases as $|c_0|^2$ decreases. Figures 10(b) and 10(c) show the experimental decays for this case.

2. *Approach to Steady State*

In an effort to reproduce the pulse shapes of Fig. 10 in the region before steady-state values are reached, we have obtained numerical solutions to the coupled nonlinear Eqs. (33) and the uniform-mode equation

$$\dot{c}_0 = -i\omega_0 c_0 - \eta_0 c_0 - i\sum_k g_{0k}^{*} c_k c_{-k} c_0^{\dagger} - iFe^{-i\omega_0 t} , \tag{46}$$

where F is a driving term proportional to h. As many as three pairs of excited spin waves $\vec{k}$, $-\vec{k}$; $\vec{k}'$, $-\vec{k}'$; and $\vec{k}''$, $-\vec{k}''$ have been considered. Frequencies $\tilde{\omega}_k$ and relaxation rates η_k are held constant during the calculation.

Spin-wave buildup cannot occur unless the initial $k \neq 0$ amplitudes are nonzero. It is possible to rewrite (33) and the similar equation for $\dot{c}_{-k}^{\dagger}$ as coupled equations for the quantities $c_k c_{-k}$, $c_k^{\dagger} c_{-k}^{\dagger}$, and $|c_k|^2 = |c_{-k}|^2$. The advantage of this is that separate initial conditions can be placed on $|c_k|^2$ and $c_k c_{-k}$. We have taken $c_k c_{-k} = 0$, $|c_k|^2 = 0.1\,|c_0|^2_{\text{crit}}$ for all $k \neq 0$ and $c_0 = |c_0| = 0$ as initial conditions. These allow for random phases at $t = 0$ and let the spin waves build up in a fairly short period of time. Since we are primarily interested in the shape of the pulse rather than absolute buildup times, the initial value of $|c_k|^2$ is not overly important.

Harker and Shaw[23] have also obtained computer solutions for spin-wave buildup and reaction back

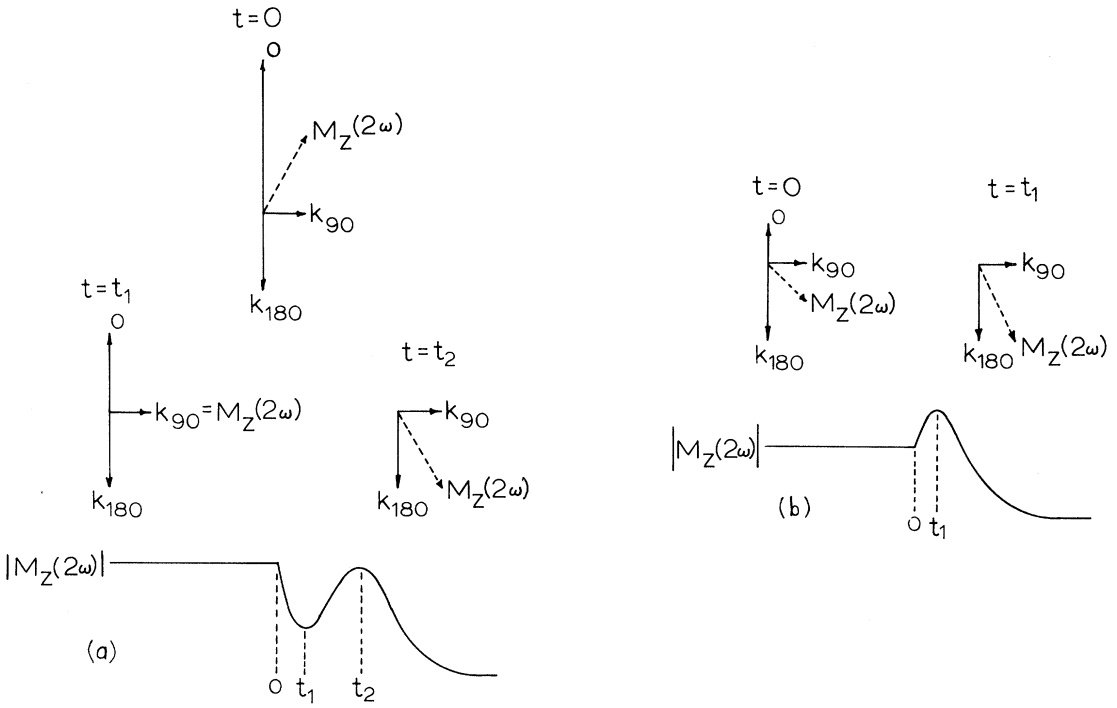

FIG. 12. Phasor diagrams for explanation of transient decay of second-harmonic pulse. O, k_{90}, k_{180} are, respectively, contribution to $M_z(2\omega)$ of uniform mode, spin waves 90° out of phase with $c_0^{\dagger 2}$, and spin waves 180° out of phase with $c_0^{\dagger 2}$. (a) $k_{180} < |c_0^{\dagger}|^2$ in steady state, (b) $k_{180} > |c_0^{\dagger}|^2$ in steady state. Incident power is turned off at $t = 0$, and uniform mode decays rapidly owing to radiation damping. Uniform-mode amplitude has become negligible in time t_2 in (a) and t_1 in (b).

on the uniform mode. They performed integrations over $\vec{k}$ space and thus included all spin waves which interact with the uniform mode, but they did not consider interactions among $k \neq 0$ spin waves as we do. That is, they solved Eqs. (3) and (46). Interaction terms $g_{kk'}$, of course, complicate matters considerably and restrict us to a small number of spin-wave pairs.

Results are shown in Fig. 13 for two and three pairs of excited spin waves. Parameters are given in the figure caption. The initial spikes agree with experiment quite well. These occur because the uniform mode can build up to a greater-than-steady-state value before the limiting effects of spin waves are manifested. Transient decays also are satisfactorily reproduced.

The main feature we had hoped to explain, however, is the pronounced second peak on the harmonic pulse [Fig. 10 (c)] which occurs after the transverse magnetization appears to have reached steady state. Comparison of Fig. 13 with Fig. 10 (c) shows that we have not had much success in this regard. We do note, though, that the curve with three spin-wave pairs shows a much longer decay of the second peak than does the one for two spin-wave pairs. This is a step in the right direction, and perhaps a model with many more interacting pairs can reproduce the experimental results. Computer time for such a calculation is likely to be prohibitive, however. Twelve minutes on a GE-625 were required for two spin-wave pairs, and 20 min for three pairs.

E. Spin-Wave Contribution to P from Transient Decay

In our previous work[14,22] we felt that the steady-state spin-wave contribution to $P_{2\omega}$, proportional to $|\sum_{k\neq 0} c_k^\dagger c_{-k}^\dagger|^2$, could be estimated by extrapolating the long-time behavior of the $P_{2\omega}$ transient back to the time at which the incident pulse is turned off. The values thus obtained were, however, considerably greater than given by theory (see Fig. 2 of Ref. 22).

The reason for this discrepancy is probably that initially after the incident pulse is turned off the spin waves decay at a rate slower than η_k because of energy supplied from the uniform mode. Not until the uniform-mode amplitude has decayed well below the threshold value can we expect the spin-wave contribution to $P_{2\omega}$ to show an $e^{-\eta_k t}$ dependence. Thus if the long-time portion of $P_{2\omega}$, which does go as $e^{-\eta_k t}$, is extrapolated back to $t = 0$ (time at which incident pulse is turned off) the resulting extrapolation will be greater than the true value at $t = 0$.

V. SUMMARY AND CONCLUSIONS

Measurements of second-harmonic power output have been performed above the second-order Suhl threshold. These show several interesting features. The steady-state power output goes through a minimum and then a maximum as incident power is increased above threshold. Dependence of $P_{2\omega}$ upon dc field H shows two and then three peaks. After the pulse of incident power is turned off, $P_{2\omega}$ initially increases. None of these curiosities is reflected in the uniform-mode behavior. The transverse magnetization always increases above threshold, shows only a single peak versus H, and decays normally.

Parametric coupling between the initial spin waves which go unstable and other $k \neq 0$ spin waves can explain the above effects. This coupling implies phase relations such that the second group of excited spin waves contributes to $P_{2\omega}$ 180° out of phase with the uniform mode. On the other hand, if all $k \neq 0$ magnon-magnon interactions are lumped into effective relaxation rates, all spin waves would contribute to $P_{2\omega}$ 90° out of phase with the uniform mode, and none of the observed anomalies would result.

We conclude that our experiments give striking evidence of the fact that the same type Suhl processes which limit uniform-mode growth also occur for the spin waves which are excited by the uniform mode. This coupling produces coherent phase relations which can be inferred from study

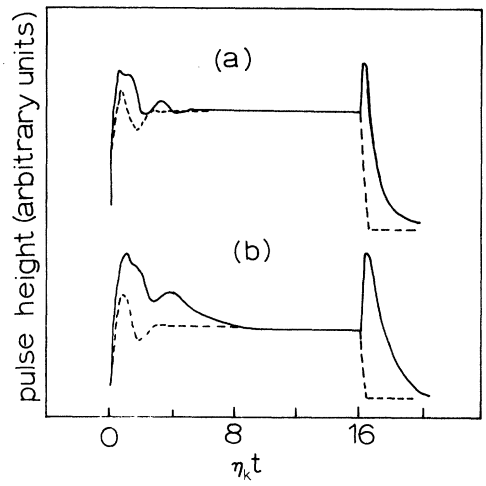

FIG. 13. Computer solutions for transverse magnetization and second-harmonic pulses. Driving field corresponds to 14 dB above threshold. Solid curves $P_{2\omega}$, dashed curves $|M_\perp(\omega)|^2$. Curves are normalized to steady-state values. (a) For two spin-wave pairs $\vec{k}, -\vec{k}$ and $\vec{k}', -\vec{k}'$ excited; $\eta_0/\eta_k = 0.8$, $\eta_{k'}/\eta_k = 0.5$, $g_{0k'}/g_{0k} = 0.5$, $g_{kk'}/g_{0k} = 0.8$. (b) For three spin-wave pairs $\vec{k}, -\vec{k}$, $\vec{k}' - \vec{k}'$, and $\vec{k}'', -\vec{k}''$ excited; $\eta_0/\eta_k = 0.8$, $\eta_{k'}/\eta_k = 0.5$, $\eta_{k''}/\eta_k = 0.4$, $g_{0k'}/g_{0k} = 0.5$, $g_{0k''} = 0$, $g_{k'k''}/g_{0k} = g_{kk''}/g_{0k} = 0.2$, $g_{kk'}/g_{0k} = 0.7$.

of harmonic generation. Analysis of the transverse resonance alone does not reveal the presence of these phase relations between $k \neq 0$ modes; so the usefulness of harmonic generation as a research tool is established.

Agreement between theory and experiment is satisfactory in most aspects. The strong second peak on the $P_{2\omega}$ pulse has not been adequately explained, however. This is an interesting effect since it shows that relatively large harmonic power outputs are possible on the front part of the pulse and for times longer than required for the transverse magnetization to reach its steady-state level. There are indications that inclusion of many spin-wave pairs in a numerical calculation may reproduce the observed pulse shape. This is based on the fact that three spin-wave pairs gives a better qualitative picture than two pairs. A second point is that the assumption of azimuthal independence of $c_k c_{-k}$, whereby one goes from (9) and (11a) to (13) may not hold, at least during the transient buildup. If, for example, spin waves with $\theta_k = \frac{1}{2}\pi$ and one definite ϕ_k were to be excited, they could make a very large contribution to $P_{2\omega}(\omega_M \approx 30B_a$ for YIG) without having a drastic effect on the transverse magnetization. Crystalline anisotropy does introduce ϕ_k dependence; so such a situation could be possible.

The effective-relaxation-rate treatment (Sec. IV A) does reproduce the transverse magnetization quite well whereas we know from the harmonic-generation data that this theory cannot be correct. Such agreement must therefore be regarded as fortuitous. Ideally the dependence of uniform-mode amplitude upon driving field should be obtained from (33) and (46) with the same parameters as required to fit the harmonic-generation data. In this way we would have a completely consistent theory. On resonance, (35) and (46) yield

$$y = x\eta_0(0)/\bar{\eta}_0 \quad , \tag{47}$$

where $\eta_0(0)$ is the uniform-mode-relaxation rate below threshold and

$$\bar{\eta}_0 = \eta_0 + \sum_{k \neq 0} g_{0k}^* |c_k|^2 \cos\Phi_k \quad . \tag{48}$$

This involves an average of $g_{0k}\cos\Phi_k$ over the distribution of excited spin waves while the average of $\cos\Phi_k$ itself is needed for $P_{2\omega}$. Also η_0 may be power dependent since it depends on the spin-wave temperature. Thus two new parameters, depending upon variation of η_0 and $\langle g_{0k}\rangle$ with power, are required; so it is not possible to predict uniform-mode behavior from the quantities α and ν alone which are needed for the $P_{2\omega}$ data.

We have attempted[14] fitting the transverse magnetization data with a two-spin-wave-pair model, but the results are not nearly as good as those obtained from Eq. (30). Thus the effective-relaxation-rate description of the uniform mode above resonance is useful if not correct.

ACKNOWLEDGMENTS

Crystal orientation was checked with x-ray apparatus of Professor R. T. Howard, Department of Metallurgy, University of Kansas. Y. H. Huang aided in construction of some of the equipment. L. W. Hinderks and K. Norland helped with the computation which was done with facilities of the University of Kansas computation center.

APPENDIX: SUHL FIRST-ORDER PROCESS

The uniform-mode amplitude stays constant above threshold when the Suhl first-order process is allowed on resonance.[1,3,4] To our knowledge there are no exceptions to this reported in the literature, and we have verified the behavior with experiments on our YIG spheres between 1.86 and 2.1 GHz (frequency must be less than 3.3 GHz for the process to be allowed on resonance in a YIG sphere at room temperature).

Why there is "sticking" for the first-order, but not for the second-order process, may be understood either in terms of the effective-relaxation rate model or explicit consideration of the parametric processes. Consider first the effective-relaxation-rate picture. We assume Eqs. (23) and (24) to hold for the first-order process with roughly the same value of C. Then since the critical value of $|c_0|^2$ for the first-order process is less than that for the second-order process by a factor of the order of $\eta_k/\omega_M \ll 1$, (26) and (27) show that the corresponding change ΔT in spin-wave temperature is much less for the first-order process. That is, much less power is involved in the first-order process; so there is not sufficient heating of the spin-wave system to cause η_k to change appreciably.

What about the initially excited spin waves being limited by parametric processes? Here we note that for the first-order process the first spin waves to go unstable have[7,8] $\theta_k = \frac{1}{4}\pi$. In the absence of anisotropy they will be excited equally in all azimuthal directions; so no one pair can acquire large amplitude as required for the parametric limiting. With the inclusion of cubic anisotropy, Schlömann[7] has shown that azimuthal invariance is preserved for $\vec{H}$ in a $\langle 100\rangle$ direction, but the coupling does vary with ϕ_k for $\vec{H}$ in the [111] direction. Even in this latter case, though, there are still six directions where the coupling constant has the same maximum value. Hence the amplitude $|c_k|^2$ for each direction is $\frac{1}{6}$ what it would be if only one pair were excited; so it is difficult for sufficiently

large spin-wave amplitudes to be attained. Also, the next spin waves excited do not have total momentum of zero, since they are produced by destruction of a single magnon $\vec{k}$. Thus energy cannot be coupled into them from the uniform mode.

For the second-order process, the first spin waves to go unstable are z directed. There is only one pair, so a large spin-wave amplitude can result. The next pair $\vec{k}'$, $-\vec{k}'$ to be excited can absorb energy from the uniform mode as long as $g_{0k'} \neq 0$, and this aids in maintaining the excitation. These considerations show why the initially excited spin waves are not likely to be limited by parametric processes when the Suhl first-order process is involved while such limiting does occur for the second-order process.

A final note is that for the initially excited spin wave to undergo a first-order parametric process one requires the existence of spin waves for which $\omega_k = \frac{1}{4}\omega_0$. For a YIG sphere at room temperature, this means the frequency must be less than 2.2 GHz. For this reason, we operated at 2.1 GHz and below. A null result at these frequencies showed, consistent with the above, that these processes do not in fact occur even when allowed by conservation of energy.

---

*Supported by the U.S. Atomic Energy Commission.

†Present address: Central Research Department, E. I. duPont de Nemours & Co., Inc., Wilmington, Del. National Science Foundation predoctoral trainee during the course of this work.

[1]H. Suhl, J. Phys. Chem. Solids 1, 209 (1957); Proc. IRE 44, 1270 (1956).

[2]N. Bloembergen and S. Wang, Phys. Rev. 93, 72 (1954).

[3]E. G. Spencer, R. C. LeCraw, and C. S. Porter, J. Appl. Phys. 29, 429 (1958).

[4]B. Desormiere, E. Milot, and H. LeGall, J. Phys. Chem. Solids 30, 1135 (1969).

[5]L. K. Anderson, Microwave Laboratory Report No. 880, Stanford University, 1962 (unpublished).

[6]In inhomogeneous samples, where two-magnon scattering is large, the susceptibility shows a gradual decline which asymptotically approaches $1/h$. This has been explained by Suhl [H. Suhl, J. Appl. Phys. 30, 1961 (1959)] and Schlömann [E. Schlömann, Phys. Rev. 116, 828 (1959)] in terms of the effects of two-magnon scattering on the nonlinear processes and is not of concern here. The susceptibility declines found in Ref. 5 and here deviate from $1/h$ in a manner which is quite unlike that expected for inhomogeneity scattering. These data were taken on well-polished YIG spheres of high purity. We thus concern ourselves solely with anomalies which would occur in a homogeneous system and do not consider two-magnon scattering.

[7]E. Schlömann, Technical Report No. R-48, Research Division, Raytheon Co., Waltham, Mass., 1959 (unpublished).

[8]R. M. White and M. Sparks, Phys. Rev. 130, 632 (1963).

[9]E. Schlömann, J. Appl. Phys. 33, 527 (1962).

[10]W. P. Ayres, P. H. Vartanian, and J. L. Melchor, J. Appl. Phys. 27, 188 (1956).

[11]P. M. Richards and H. J. Shaw, Phys. Rev. Letters 8, 202 (1962); J. Appl. Phys. 35, 187 (1964).

[12]T. Holstein and H. Primakoff, Phys. Rev. 58, 1098 (1940).

[13]For a clear introduction to the Holstein-Primakoff transformation and other formalism used here, the reader is referred to the text by M. Sparks, *Ferromagnetic Relaxation Theory* (McGraw-Hill, New York, 1964).

[14]J. D. Bierlein, Ph.D. thesis, University of Kansas, 1967 (unpublished).

[15]E. L. Ginzton, *Microwave Measurements* (McGraw-Hill, New York, 1957), p. 407.

[16]T. J. Matcovich, H. S. Belson, N. Goldberg, and C. W. Haas, J. Appl. Phys. 33, 1287 (1962).

[17]M. T. Weiss, Phys. Rev. Letters 7, 239 (1958); G. E. Bodway and S. Wang, J. Appl. Phys. 36, 2566 (1965).

[18]E. Schlömann, J. J. Green, and U. Milano, J. Appl. Phys. Suppl. 31, 386 (1960).

[19]F. R. Morgenthaler, J. Appl. Phys. Suppl. 31, 95 (1960).

[20]M. Sparks, R. Loudon, and C. Kittel, Phys. Rev. 122, 791 (1961).

[21]E. Schlömann, J. Appl. Phys. 33, 527 (1962).

[22]J. D. Bierlein, L. W. Hinderks, and P. M. Richards, J. Appl. Phys. 38, 1232 (1967).

[23]K. J. Harker and H. J. Shaw, J. Appl. Phys. 37, 3035 (1966).

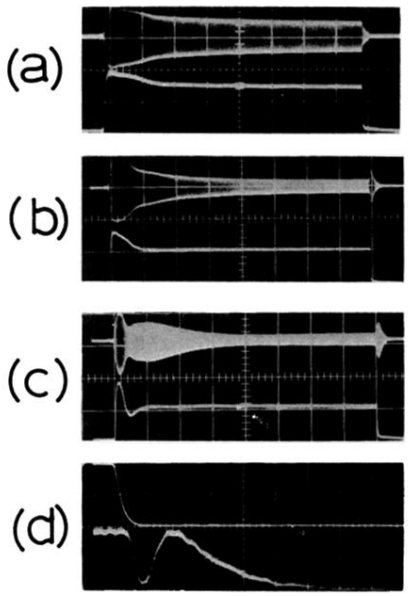

FIG. 10. Second-harmonic and transverse magnetization pulse shapes (a) 6 dB above threshold, 1 μsec/cm; (b) 9.6 dB above threshold, 1 μsec/cm; (c) 14 dB above threshold, 1 μsec/cm; (d) 8 dB above threshold, 50 nsec/cm. In (a)–(c) the upper trace is second-harmonic (if envelope) and the lower trace transverse magnetization. In (d) the lower trace is second-harmonic (straight video detection) and the upper trace transverse magnetization.